Supplementary information:

Pure and Sb-doped ZrO2 for removal of IO_3^- from radioactive waste solutions

Running title: ZrO_2 materials for IO_3^- removal

V. Suorsa[1,*], M. Otaki [1], J. Virkanen[2] and R. Koivula[1]

[1] *Radiochemistry Unit, Department of Chemistry, University of Helsinki, A.I. Virtasen aukio 1, 00014 Helsinki, Finland*

[2] *Department of Geosciences and Geography, University of Helsinki, Gustaf Hällströmin katu 2, 00014 Helsinki, Finland*

** Corresponding author. E-mail address: valtteri.suorsa@helsinki.fi; ORCID: 0000-0003-1544-5283*

Abstract

Radioactive ^{129}I with a long half-life (1.57×10^7 y) and high mobility is a serious radiohazard and one of the top risk radionuclides associated to its accidental and planned releases to nature. The complex speciation chemistry of iodine makes its removal a complicated task and usually a single method is not able to remove all iodine species. Especially its oxidized form iodate (IO_3^-) lacks a selective and effective removal method. Here the granular aggregates of hydrous zirconium oxides with and without antimony doping were tested for IO_3^- removal and the effects of contact time, competing anions in different concentrations and pH were examined. The materials showed high selectivity for IO_3^- (K_d over up to 50000 ml/g) in the presence of competing ions and relatively fast uptake kinetics (eq. < 1h). However, $B(OH)_4^-$ and SO_4^{2-} , as competing ions, lowered the iodate uptake significantly in basic and acidic solution, respectively. The suitability of the materials for practical applications was tested in a series of column experiments where the materials showed remarkably high apparent capacity for the IO_3^- uptake (3.2 – 3.5 mmol/g).

1. Characterization

The surface morphologies of the materials coated with 4 nm Au-Pd sputtering were examined using Hitachi S4800 FE-SEM (field-emission scanning electron microscopy).

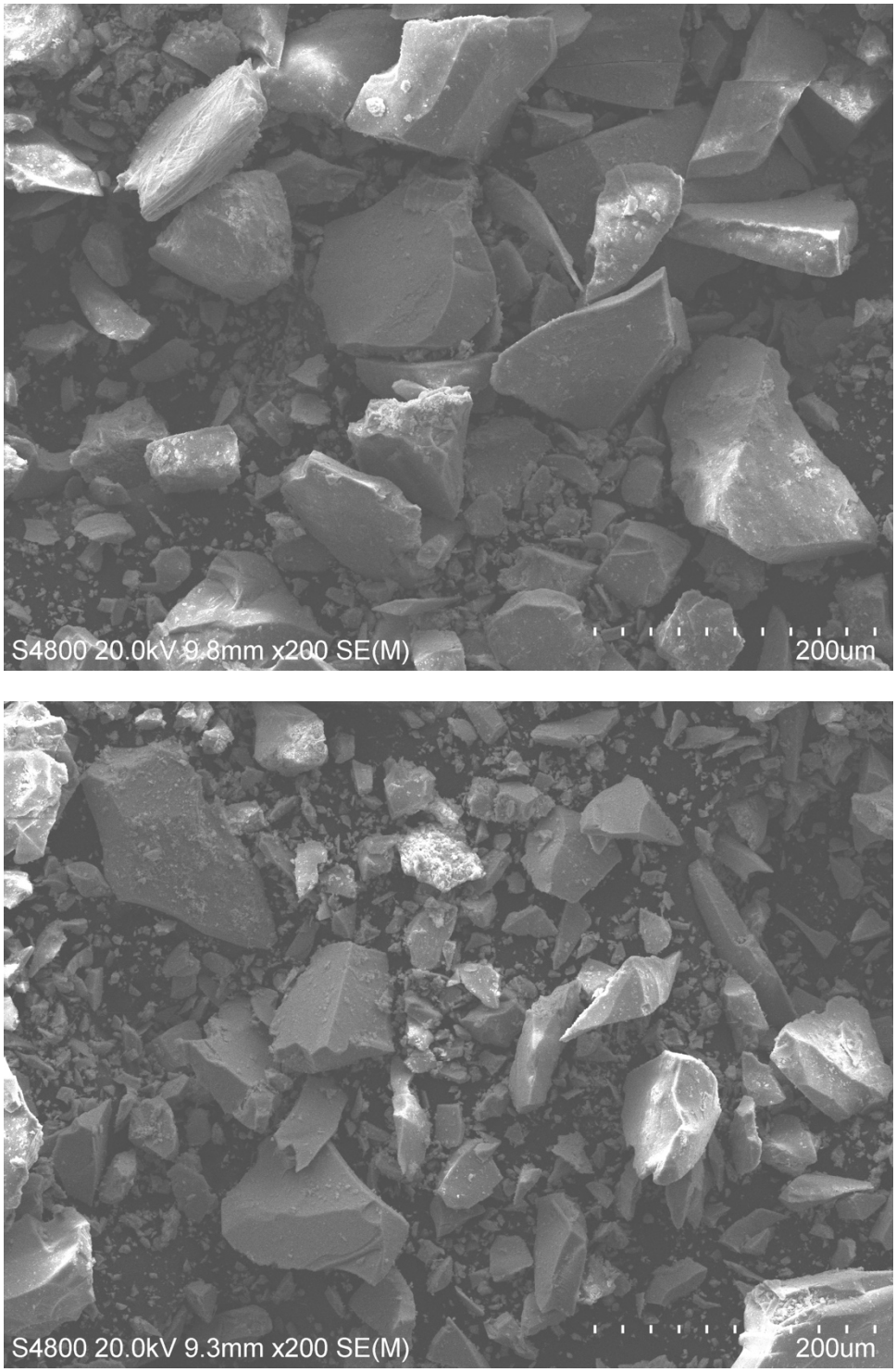

Fig 1 SEM images of the two materials after drying. $ZrSbO_2$ is shown in the upper figure, ZrO_2 in the lower.

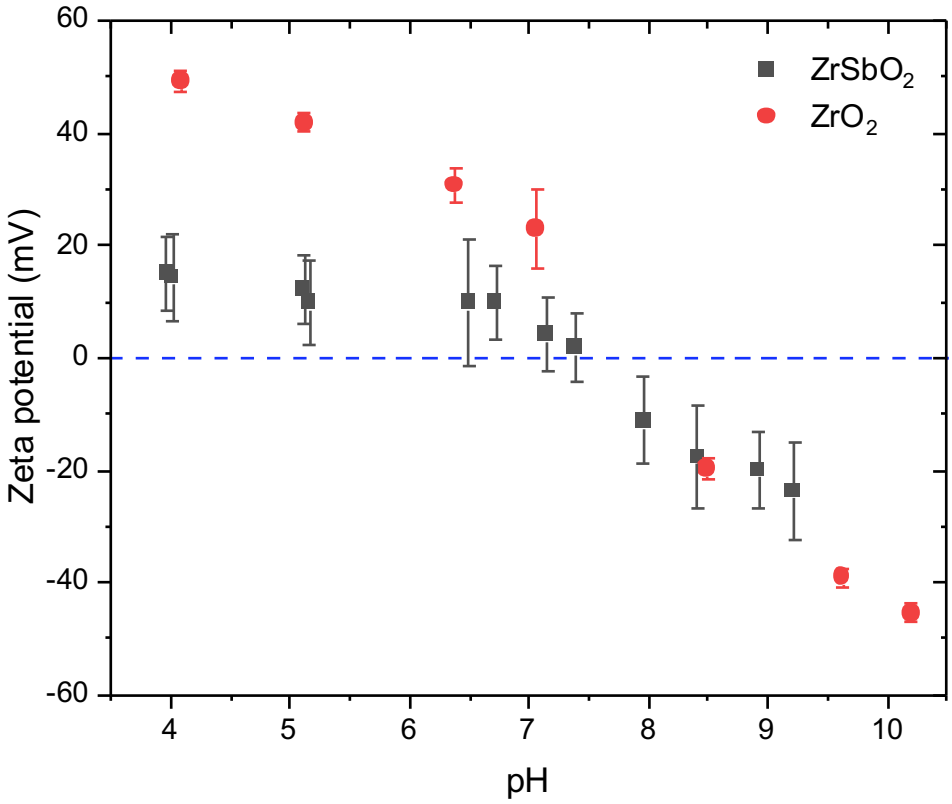

Fig 2 The apparent Zeta potentials as functions of equilibrium pH for 20 mg ZrO_2 and $ZrSbO_2$ in 10 ml of 10 mM $NaNO_3$. The dashed blue horizontal line shows the zero value to guide the reader's view. The results are given as the mean value of repeated measurements and the standard deviation for each sample are shown as error bars.

2. Verification of iodine speciation of ^{125}I and ^{127}I

The speciation of iodine is primarily depending on solution's redox potential and pH. In general, iodate (IO_3^-), is dominant species in oxidizing environments, while iodide (I^-) becomes the main species in more reducing conditions. In addition, in extremely low pH molecular iodine (I_2) becomes stable. The speciation of iodine affects crucially its behaviour and interactions with different materials. In the experiments of this study, the behaviour of iodate was the main concern.

In the case of non-radioactive ^{127}I, the iodine speciation was confirmed by using an anion-exchange chromatography column (Dionex AS11 4 x 250 mm analytical column and AG11 4 x 50 mm guard column) attached to an Agilent 1260 Infinity quaternary pump and autosampler HPLC-system connected to an

Agilent 7800 ICP-MS via direct connection between the column and ICP nebulizer. The two main species of iodine I^- and IO_3^- were separated based on their retention times, first determined with standard solutions prepared from KI and KIO_3, and the concentrations were calculated from the chromatogram peak areas using external standards on the concentration range from 0 to 200 μg L^{-1} for both iodine species.

The speciation of $^{125}IO_3^-$ was confirmed with repeated simple batch experiments done for tracer solutions where silver-impregnated activated charcoal (Silcarbon Aktivkohle GmbH, Germany) was used to quantify the iodate fraction. (Suorsa, Otaki, Zhang, Virkanen, & Koivula, 2020). In 10 mM $NaNO_3$ solution, the silver impregnated activated charcoal has strong affinity to iodide but minimal to iodate (K_D: IO_3^- ~ 0 ml/g ; I^-: ~ 10^5 ml/g). Low distribution coefficients with SilCarbon indicate low I^- content in solution. Limit was set so that K_D's with $^{125}IO_3^-$ tracer should be less than 50 ml/g for SilCarbon to indicate successful oxidation to iodate form. Wallac 1480 Wizard 3" automated NaI-scintillation γ-detector was used to measure the $^{125}IO_3^-$ radioactivity in the samples. Fig 3 shows the adsorption of ^{125}I to silver-impregnated activated carbon (Silcarbon Aktivkohle GmbH, Germany) for the different stock solutions used within the experiments. The procedure has been previously validated for alteration and separation of oxidation states of iodine (Suorsa, Otaki, Zhang, Virkanen, & Koivula, 2020).

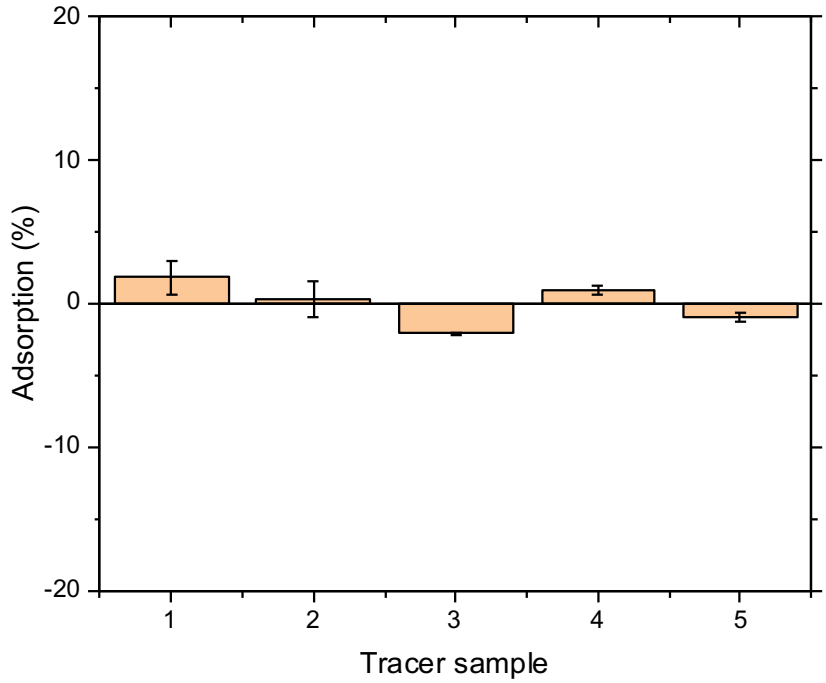

Fig 3 The adsorption of radioactive ^{125}I to 20 mg of silver-impregnated activated carbon (Silcarbon Aktivkohle GmbH, Germany) in 10 mL of 10 mM $NaNO_3$ (pH 7). In the case of I^- the adsorption is 100% because of formation of insoluble AgI. In the case of IO_3^- low adsorption is observed. The total iodine concentrations were in the range of ~ 10^{-13} M.

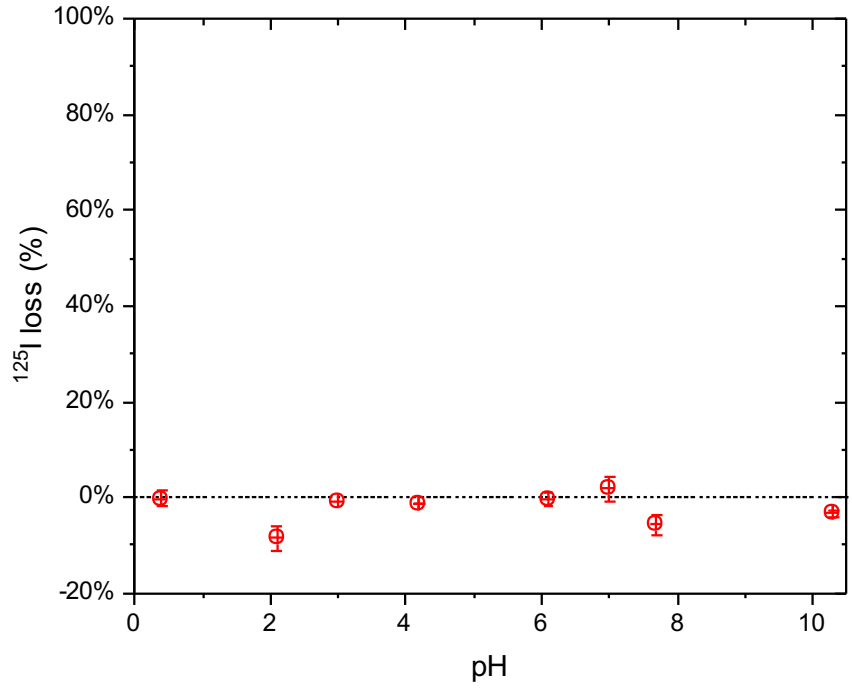

Fig 4 $^{125}IO_3^-$ loss without any material as function of pH in 10 mM $NaNO_3$ solution. The error bars show standard deviation of two parallel samples.

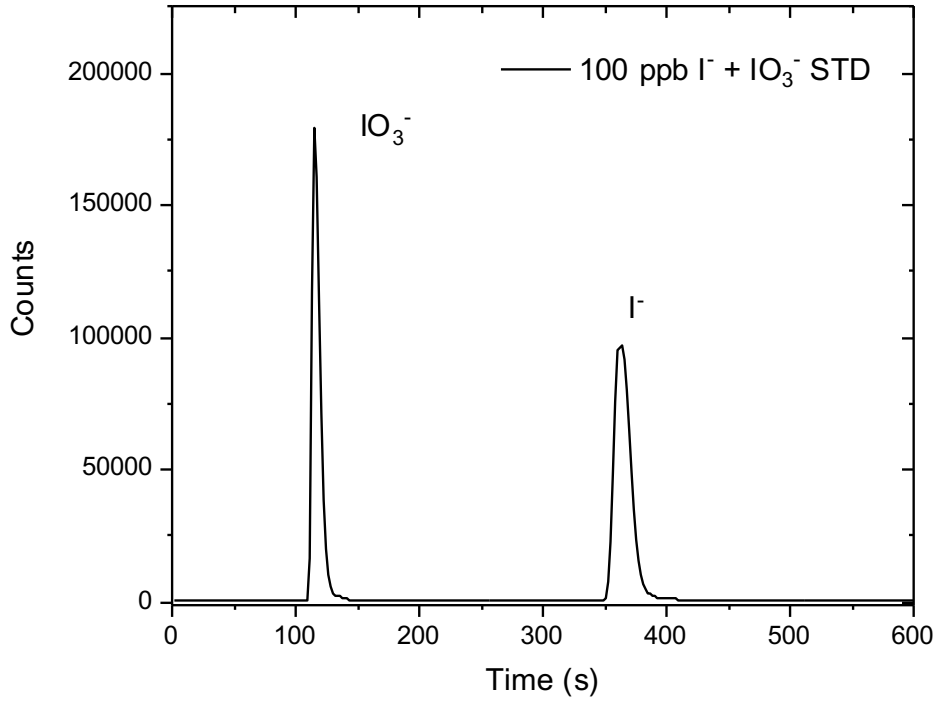

Fig 5 An example chromatogram of a standard sample containing 100 ppb of both I^- and IO_3^-.

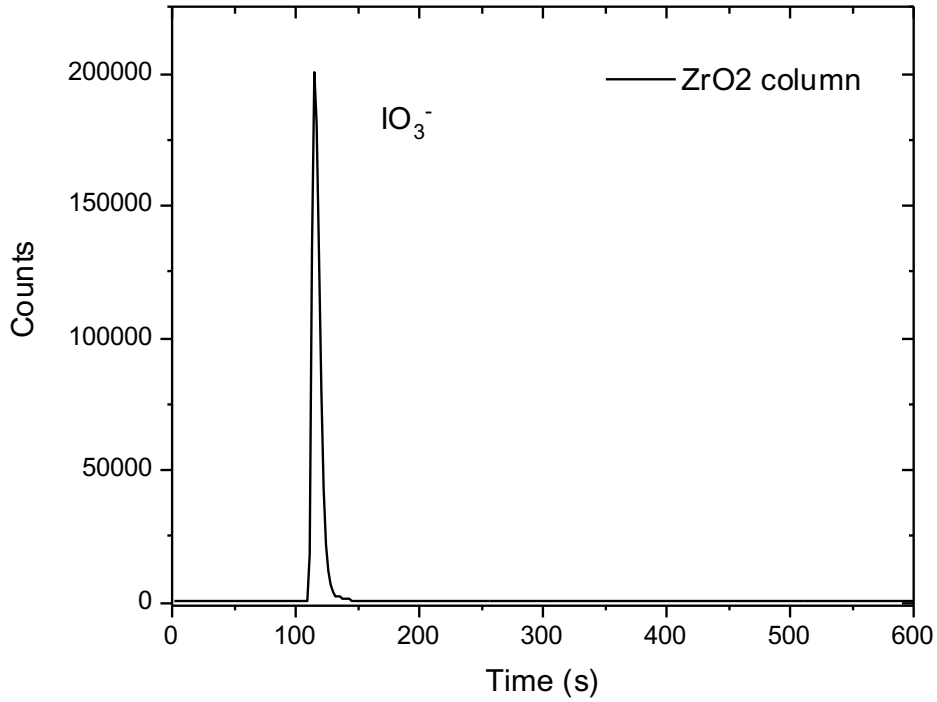

Fig 6 An example chromatogram of ZrO_2 column effluent from the column experiment 2 showing only the IO_3^- peak indicating that no redox changes have occured in the solution phase.

3. Batch experiments

Calculations and equations

The distribution coefficients, K_d's, in the batch experiments were calculated by Eq. 1.

$$K_d = \frac{c_i - c_f}{c_f} \times \frac{V}{m} \quad (1)$$

where

c_i = initial concentration of iodate in the solution.
c_f = final concentration of iodate in the solution.
V = volume of solution in mL
m = mass of material in g

In Eq. 1 $\frac{V}{m}$ can be replaced by batch factor BF (mL g^{-1}) giving the equation the final form shown in Eq. 2.

$$K_d = \frac{c_i - c_f}{c_f} \times BF \quad (2)$$

The errors of independent K_d values were calculated with the propagation of error and by using the final equation Eg. 3. The equation does not take into account the error of pipette (0.2 %) or scale (0.05 %), but which are low compared to the error of concentration measurement (relative errors (1 σ) 0.5 – 50 % depending on the count rate for γ-detector; 8 % HPLC-ICP-MS).

$$\Delta K_d = \sqrt{\left(\frac{c_i \times BF}{{c_f}^2} \times \Delta c_f\right)^2 + \left(\frac{BF}{c_f} \times \Delta c_i\right)^2} \quad (3)$$

The sorption percentages were calculated by Eq. 4 and the errors of independent results by Eq. 5. The concentrations were either measured by HPLC-ICP-MS for ^{127}I or automated NaI-scintillation γ-detector for ^{125}I.

$$S\% = \frac{c_i - c_f}{c_i} \times 100\% \quad (4)$$

where

c_i = initial concentration of iodate in the solution.
c_f = final concentration of iodate in the solution.

$$\Delta S\% = \sqrt{\left(-\frac{1}{c_i} \times \Delta c_f\right)^2 + \left(\frac{c_f}{c_i} \times \Delta c_i\right)^2} \times 100\% \quad (5)$$

where

c_i = initial concentration of iodate in the solution.
c_f = final concentration of iodate in the solution.

In the most figures in the main article the error bars are representing the standard deviation of parallel samples calculated using the sample standard deviation given below in Eq. 6.

$$\Delta S\% = \sqrt{\frac{\sum_{i=0}^{n}(x_i - \bar{x})^2}{n-1}} \quad (6)$$

where

x_i = initial concentration of iodate in the solution.
$\bar{x}$ = final concentration of iodate in the solution.
n = number of samples.

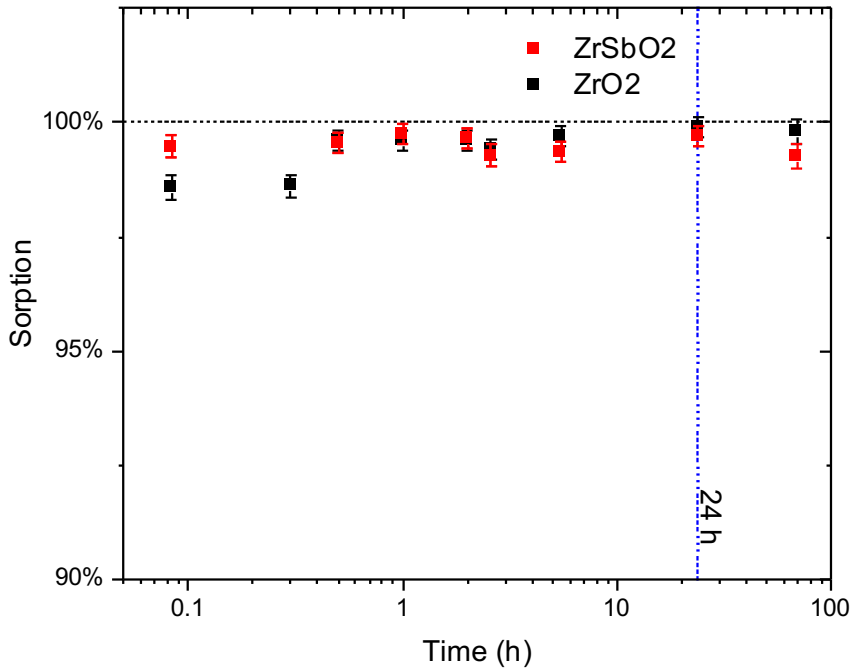

Fig 7 The adsorption of IO_3^- in 10 mM $NaNO_3$ solution on $Zr(Sb)O_2$ (black symbols) and on pure ZrO_2 (red symbols) as a function of time without pH adjustment (pH ~3.5, see SI for detailed presentation). The results show the adsorption percentage calculated as a mean of parallel samples (n = 2). The error bars represent the error (2σ) of sorption-% calculated by the propagation of uncertainty from the error of radioactivity measurement (see SI for more information).

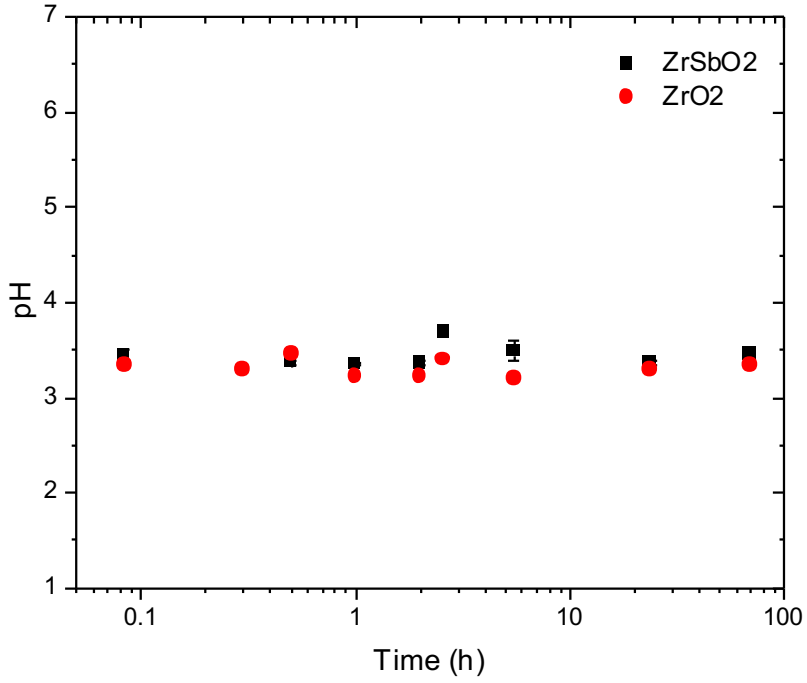

Fig 8 The pH evolution of batch samples of adsorption kinetics experiment.

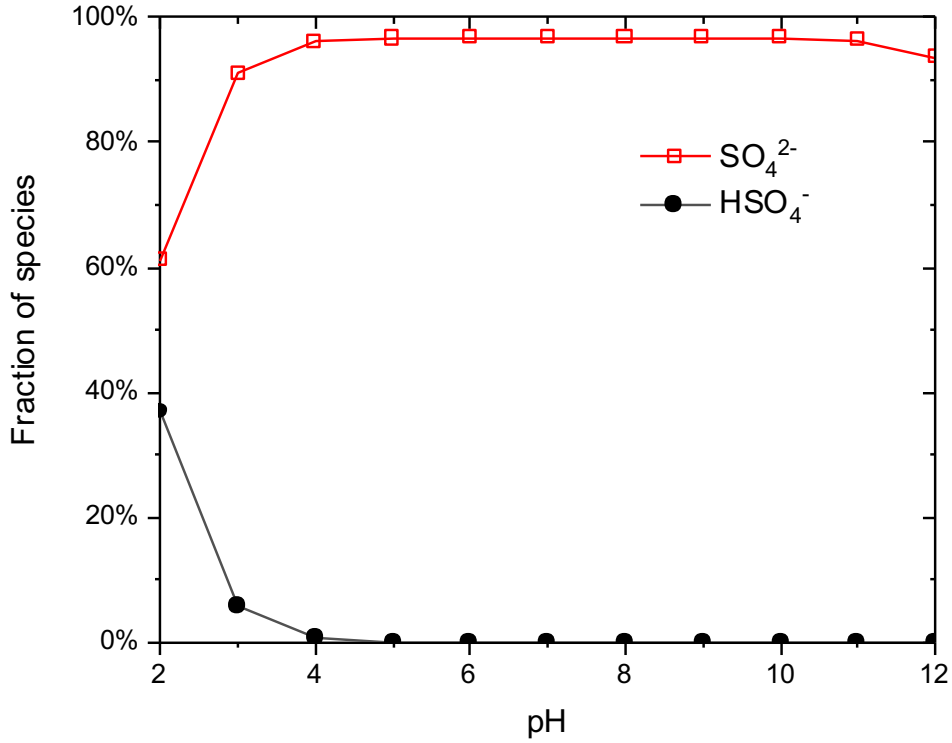

Fig 9 Solution species of sulphur (10 mM) as a function of pH calculatted with PhreeqC (Parkhurst and Appelo, 1999) using LLNL database.

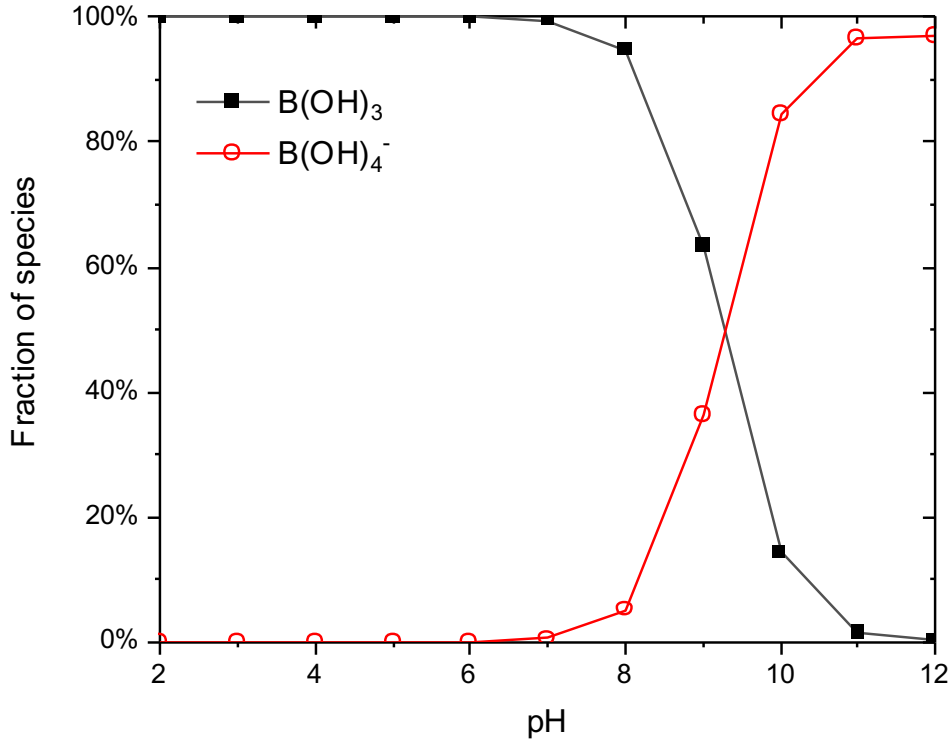

Fig 10 Solution species of boron (10 mM) as a function of pH calculatted with PhreeqC (Parkhurst and Appelo, 1999) using LLNL database.

4. Column experiments

Calculations and equations

The breakthrough percentages were calculated by Eq. 7.

$$Breakthrough\% = \frac{c_f}{c_i} \times 100\% \quad (7)$$

where

c_f = concentration of iodate in the effluent sample.

c_i = concentration in feed solution.

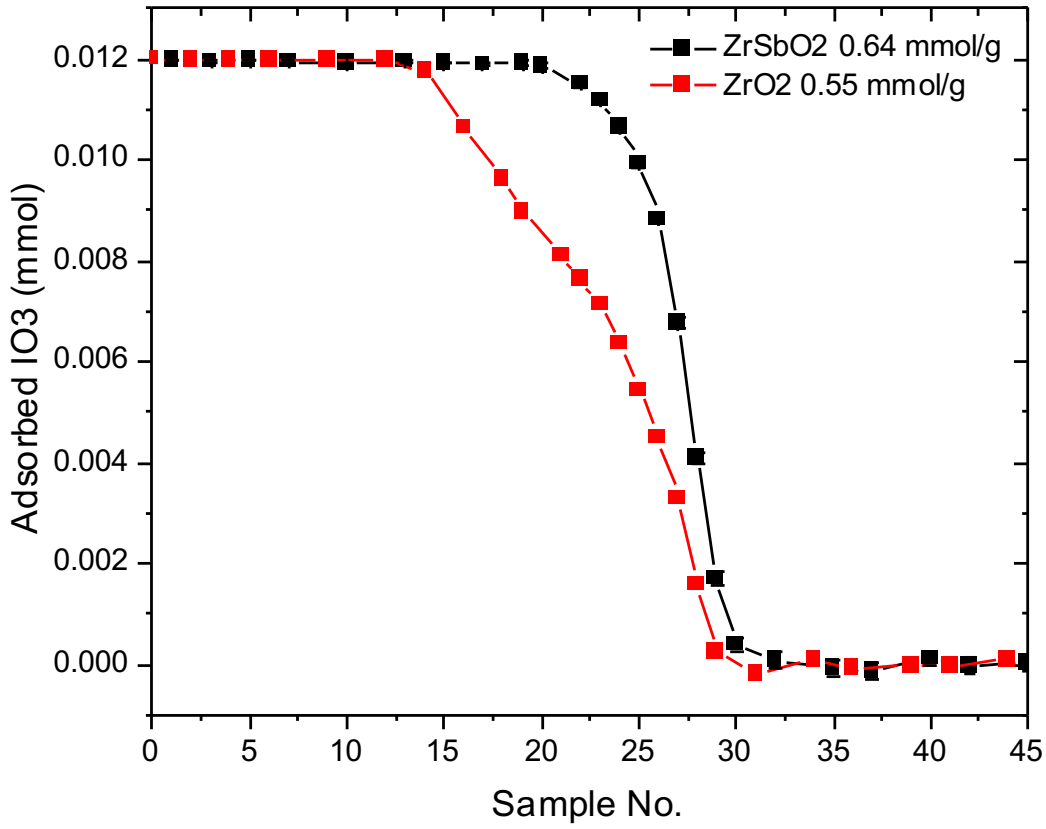

Fig 11 Adsorbed iodate in mmols per individual sample. The apparent capacity was calculated by integrating the area below the graph with OriginPro 2020.

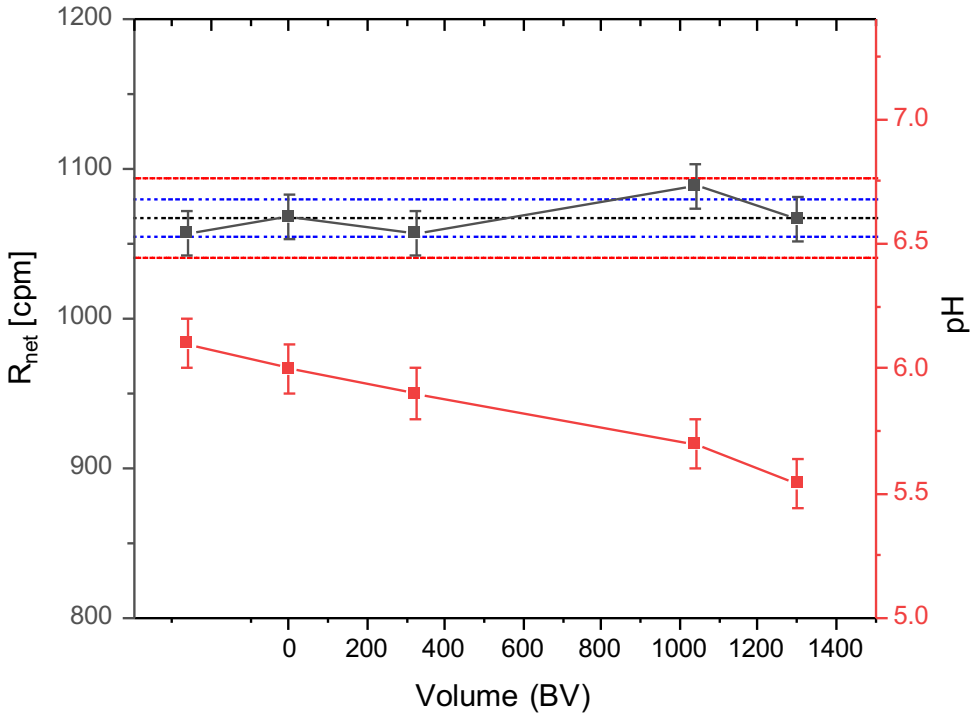

Fig 12 Stability of the feed solution of column experiment No. 2 done with 10 mM $NaNO_3$ solution. The R_{net} (black dots and left axis) show the counts per minute for 5 mL samples of feed solution taken at appropriate interval and measured at the same time after the experiment. The pH of feed solution samples (red dots and right axis) show slight pH drop from 6.0 to 5.5 was probably due the atmospheric CO_2.

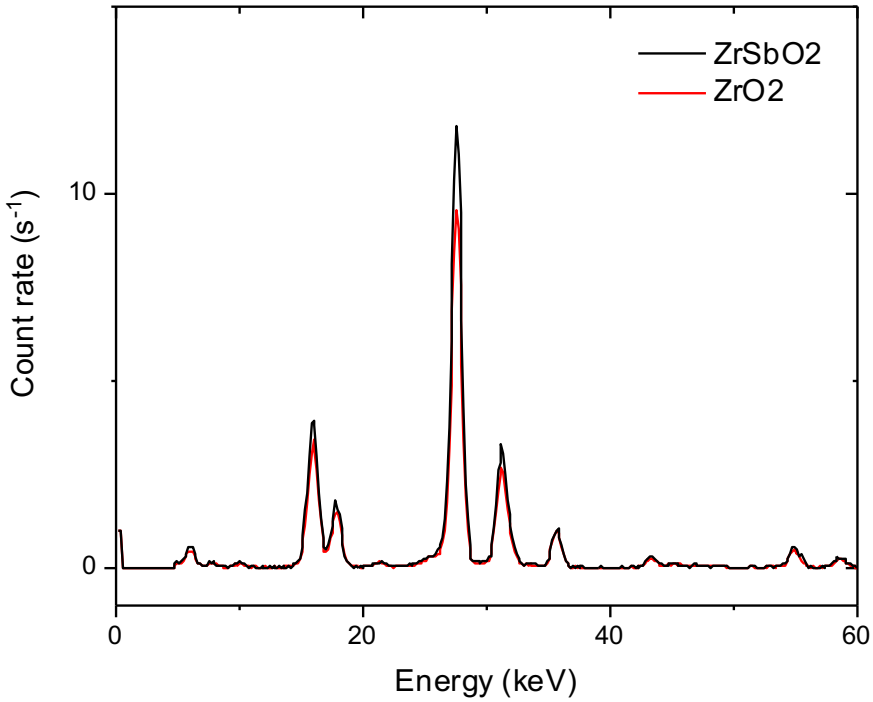

Fig 13 The gamma spectrum of the IO3- loaded columns after the experiment. The data is qualitative only as ZrO_2 is absorbing a large fraction of the gamma rays at the low energy region of ^{125}I.

Acknowledgements

Financial support from the Doctoral Programme in Chemistry and Molecular Sciences (CHEMS) at the University of Helsinki is gratefully acknowledged. The authors gratefully appreciate the help in batch and column experiments by Ms Susanna Heikkilä.

References

Suorsa, V.; Otaki, M.; Zhang, W.; Virkanen, J.; Koivula, R. A simple method for quantifying iodate and iodide fractions in solution using Ag -impregnated activated carbon. J. Radioanal. Nucl. 2020, 1-8. https://doi.org/10.1007/s10967-020-07061-4

Parkhurst D.L. and Appelo C.A.J. (1999) User's guide to PHREEQC (version 2) – A computer program for speciation, batch-reaction, one-dimensional transport and inverse geochemical calculations. Water-Resources Investigations Report 99-4259. Denver, Colorado.